Delayed protection by ESAT-6–specific effector CD4+ T cells after airborne *M. tuberculosis* infection

Alena M. Gallegos, Eric G. Pamer, and Michael S. Glickman

Infectious Diseases Service, Immunology Program, Memorial Sloan-Kettering Cancer Center, New York, NY 10032

***Mycobacterium tuberculosis* infection induces complex CD4 T cell responses that include T helper type 1 (Th1) cells and regulatory T cells. Although Th1 cells control infection, they are unable to fully eliminate *M. tuberculosis*, suggesting that Th1–mediated immunity is restrained from its full sterilizing potential. Investigation into T cell–mediated defense is hindered by difficulties in expanding *M. tuberculosis*–specific T cells. To circumvent this problem, we cloned CD4+ T cells from *M. tuberculosis*–infected B6 mice and generated transgenic mice expressing a T cell receptor specific for the immunodominant antigen early secreted antigenic target 6 (ESAT-6). Adoptively transferred naive ESAT-6–specific CD4+ T cells are activated in pulmonary lymph nodes between 7 and 10 d after aerosol infection and undergo robust expansion before trafficking to the lung. Adoptive transfer of activated ESAT-6–specific Th1 cells into naive recipients before aerosol *M. tuberculosis* infection dramatically enhances resistance, resulting in 100-fold fewer bacteria in infected lungs. However, despite large numbers of Th1 cells in the lungs of mice at the time of *M. tuberculosis* challenge, protection was not manifested until after 7 d following infection. Our results demonstrate that pathogen–specific Th1 cells can provide protection against inhaled *M. tuberculosis*, but only after the first week of infection.**

CORRESPONDENCE
Eric G. Pamer:
pamere@mskcc.org
OR
Michael S. Glickman:
glickman@mskcc.org

Abbreviations used: BCG, Bacille Calmette-Guérin; ESAT-6, early secreted antigenic target 6; pLN, pulmonary LN; tg, transgenic.

Mycobacterium tuberculosis is an inhaled pathogen that primarily infects macrophages and DCs. Bacterial replication in infected cells is inhibited by the actions of IFN-γ and TNF-α, supplied by antigen-specific T cells and cells of the innate immune system (1–5). Although infected humans and mice generate *M. tuberculosis*–specific T cells, the immune system is generally incapable of providing sterilizing immunity against this pathogen, and individuals cured of primary *M. tuberculosis* infection remain vulnerable to reinfection (6–8). The only approved vaccine against *M. tuberculosis*, the *M. bovis* derivative Bacille Calmette-Guérin (BCG), induces, at best, only partial immunity (9). Immunization of mice with BCG induces protective immunity that results in ∼10-fold fewer *M. tuberculosis* organisms in the lungs upon aerosol challenge.

CD4+ T cells play a dominant role in immunity to *M. tuberculosis* because animals deficient in these cells are more susceptible to infection than normal mice or mice lacking CD8+ T cells (10–12), and patients with CD4 T cell deficiency

from HIV infection have dramatically elevated rates of reactivation tuberculosis (13). After aerosol infection in mice, *M. tuberculosis* replication is controlled when effector T cells reach the lung (6). Among CD4+ T cell subsets, IFN-γ–producing Th1 cells are essential, because humans with defects in the IFN-γ receptor have markedly increased susceptibility to mycobacterial infections, and mice lacking either IFN-γ or its receptor die rapidly after infection (2–4). Although it is commonly assumed that vaccines that elicit larger or more Th1-focused antigen-specific T cell responses will be more effective, the extent to which very high numbers of *M. tuberculosis*–specific Th1 cells can provide protective immunity remains unclear.

Two hypotheses have been proposed to explain how *M. tuberculosis* evades T cell–mediated immune defenses. The first posits that *M. tuberculosis* induces complex T cell responses comprising

The online version of this article contains supplemental material.

Th1 and Th17 effector cells that enhance bacterial clearance, and regulatory T cells that restrict bacterial clearance (14–16). In this scenario, regulatory T cell function is sufficient to prevent clearance of primary infection or development of protective immunity. The second hypothesis is that *M. tuberculosis* has acquired mechanisms to hide from the immune system within infected cells, out of reach of the adaptive immune system. These hypotheses are not mutually exclusive and evidence in support of both is mounting. Because tuberculosis is a lengthy infection, with clinically distinct phases, it is likely that the mechanisms of immune evasion differ during early, latent, and late infection. Determining the relative contributions of distinct immune evasion mechanisms is essential for vaccine design and new therapeutic approaches.

In this study, we investigated whether high numbers of *M. tuberculosis*–specific Th1 cells can protect mice from infection. We generated mice that are transgenic (tg) for an MHC class II–restricted TCR specific for the *M. tuberculosis* antigen early secreted antigenic target 6 (ESAT-6). We show that ESAT-6–specific Th1 cells are remarkably potent in protecting mice from infection. However, ESAT-6–specific Th1 cells controlled bacterial replication only after day 7 following infection, despite the fact that high numbers of these cells were in the lung before, during, and after inhalation of live *M. tuberculosis*. These studies indicate that during the first week of infection, *M. tuberculosis*–infected cells are either physically inaccessible to pathogen-specific effector CD4$^+$ T cells or are functionally incapable of receiving CD4$^+$ T cell help.

RESULTS

Generation of ESAT-6–specific TCR tg mice

ESAT-6 is a secreted protein implicated in *M. tuberculosis* pathogenesis (17) and is a key antigen in humans, primates, and mice, and vaccination with ESAT-6 induces protective CD4$^+$ T cell immunity (18–22). To study the CD4$^+$ T cell response to *M. tuberculosis*, tg mice for an MHC class II–restricted TCR specific for ESAT-6$_{3-15}$ in the context of I-A^b were generated. To isolate a TCR that is functional during in vivo infection, CD4$^+$ T cells specific for ESAT-6 were harvested from mice that were aerosol infected with *M. tuberculosis*, and CD4$^+$ T cell hybridomas were generated. The specificity of one ESAT-6–specific hybridoma, clone 7, is shown in Fig. 1 A. The TCR used by clone 7 CD4$^+$ hybridoma cells was composed of a TCR β chain generated from Vβ10b-Dβ1-Jβ2.4 gene segments and a TCR α chain generated from Vα11.2-Jα27 gene segments (unpublished data). TCR α and β chain cDNAs were cloned into the VA hCD2 cassette vector, which uses the human CD2 promoter to drive the expression of cDNAs in T cells (23).

Because the TCR used to generate ESAT-6–specific TCR tg mice (referred to hereafter as C7 TCR tg mice) was isolated from a CD4$^+$ T cell, an increased frequency of this lineage in tg animals was expected. In both thymocytes and splenocytes, an increased percentage of CD4$^+$ T cells with a concomitant decrease in the frequency of CD8$^+$ T cells was observed (Fig. 1 B). The majority of CD4$^+$ thymocytes and splenocytes expressed the transgene-encoded TCR α and β chain (Fig. 1 C).

To confirm the specificity of these cells, CD4$^+$ T cells were purified from C7 TCR tg mice or B6 control animals and were stimulated with titrating amounts of ESAT-6 peptide. Although both CD4$^+$ T cell populations proliferated similarly to anti-CD3/CD28 stimulation (not depicted), only C7 TCR tg CD4$^+$ T cells proliferated in response to ESAT-6 peptide (Fig. 1 D). In summary, C7 TCR tg mice contain CD4$^+$ T cells that express a TCR specific to ESAT-6$_{3-15}$–I-A^b complexes. This TCR was isolated from a CD4$^+$ T cell clone responding to a live *M. tuberculosis* infection.

C7 TCR tg CD4$^+$ T cells differentiate into Th1 cells during *M. tuberculosis* infection

To determine whether C7 TCR tg CD4$^+$ T cells respond to ESAT-6 antigen generated during aerosol infection of mice, 10^4 naive C7 TCR tg CD4$^+$ T cells (on a RAG-1–deficient [RAG$^{-/-}$] background) were adoptively transferred into B6 recipients that were aerosol infected 1 d later with 100 CFU *M. tuberculosis*. The data in Fig. 2 A show that at this T cell dosage, naive C7 CD4$^+$ T cells (congenically marked with CD90.1) are not detectable in uninfected mice. In contrast, marked expansion of C7 CD4$^+$ T cells is noted in the pulmonary LNs (pLNs) of mice infected 12 d earlier (Fig. 2, A and B). Analysis of pLNs, spleen, and lung between days 12 and 18 of infection demonstrates that the frequency of C7 CD4$^+$ T cells increases in the lung and spleen (Fig. 2 C). Staining for intracellular TNF-α and IFN-γ demonstrates that responding C7 CD4$^+$ T cells acquired Th1 effector cell functions (Fig. 2 D). The differentiation of responding cells into Th1 effector cells is further supported by their expression of T-bet, as measured by intracellular staining (Fig. 2 E). In contrast, naive C7 CD4$^+$ T cells did not differentiate into regulatory T cells because the transcription factor Foxp3 was not expressed (unpublished data).

These experiments demonstrate that naive C7 CD4$^+$ T cells are activated in vivo in the setting of pulmonary *M. tuberculosis* infection and that they traffic from draining LNs to the lung. Furthermore, these studies demonstrate that naive C7 TCR tg CD4$^+$ T cells differentiate into Th1 effector cells, as is observed with polyclonal ESAT-6–specific T cell responses (24).

T cell priming occurs between days 7 and 10 after infection

The ESAT-6–specific CD4$^+$ T cell response to *M. tuberculosis* has been measured in functional ways via ELISA, ELISPOT, or intracellular cytokine staining in mice with a complex TCR repertoire (24, 25). One limitation of relying on these methods is that the frequency of antigen-specific cells needs to be high enough to detect by fluorimetric analysis, and these cells need to produce cytokines to be detected. Accordingly, naive cells cannot be studied because these cells need to expand and differentiate into cytokine-producing cells before they can be visualized. Using these methods, *M. tuberculosis*–specific effector CD4$^+$ T cells are first detectable in the pLNs ∼14 d

after infection, and these cells reach peak numbers in the lungs between 21 and 28 d after infection (24–26). Because the delay in recruitment of effector cells to the lung is not a general characteristic of pulmonary infections, we wanted to determine the kinetics of priming of ESAT-6–specific CD4^{+} T cells (27, 28).

To understand when naive ESAT-6–specific CD4^{+} T cells are first presented antigen after aerosol infection with *M. tuberculosis*, 10^5 CFSE-labeled naive C7 TCR tg.RAG^{−/−} CD4^{+} T cells (CD90.1) were transferred into B6 recipients (CD90.2), and recipient mice were infected 1 d later with 100 CFU *M. tuberculosis*. At days 7, 10, and 13 after infection, pLNs were recovered and the frequency and phenotype of C7 CD4^{+} T cells were determined. At day 7 after infection, the frequency of C7 CD4^{+} T cells in the pLNs was low and similar to that seen in uninfected animals. C7 CD4^{+} T cells at day 7 had a naive phenotype. These cells were CFSE bright, CD69 negative, CD44 intermediate, and CD62L high (Fig. 3 A

and not depicted). The naive phenotype of these cells, with low surface expression of the early activation marker CD69, indicates that C7 CD4^{+} T cells had not been presented antigen at the day 7 time point. By day 10 after infection, the frequency of C7 CD4^{+} T cells among CD4^{+} T cells increased compared with day 7, and every mouse examined contained either recently activated cells (expressing CD69) or divided cells, as indicated by CFSE dilution. At day 13 after infection, the frequency of the C7 CD4^{+} T cells increased to ∼6% of total CD4^{+} T cells. These cells were mostly CFSE negative and displayed an effector/memory-like cell-surface phenotype, expressing high levels CD44 and low levels of CD62L (Fig. 3 A and not depicted). The temporal change in frequency of C7 CD4^{+} T cells among the CD4^{+} T cells in the pLNs is shown in Fig. 3 B. These experiments indicate that the priming of naive ESAT-6–specific CD4^{+} T cells is delayed compared with other respiratory infections and occurs between days 7 and 10 after infection.
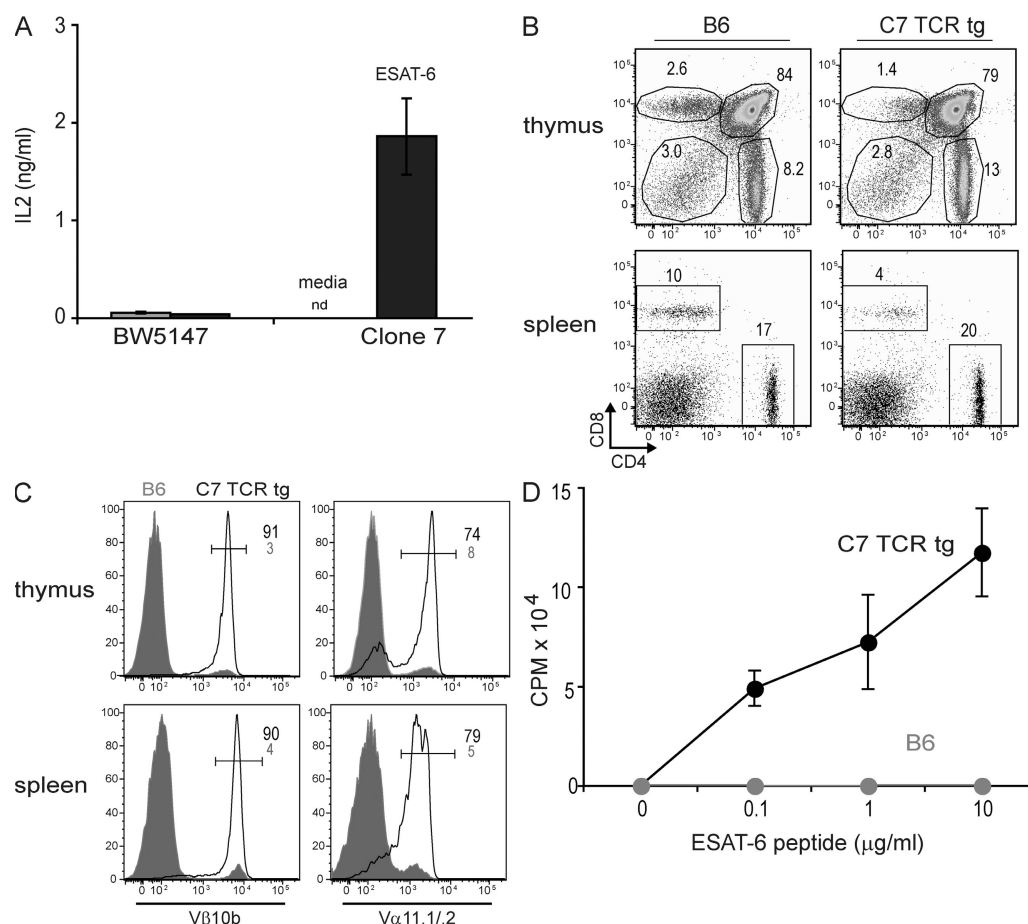
Figure 1. C7 TCR tg CD4^{+} T cells are specific to ESAT–6. (A) Clone 7 hybridoma cells or hybridoma fusion partner BW5147 cells were stimulated with 5 μg/ml of ESAT-6 peptide, or with media in the presence of APCs. Supernatants were collected 2 d later, and IL-2 levels were measured by ELISA. nd, not detectable. (B) Splenocytes and thymocytes from B6 or C7 TCR tg mice were stained for CD4 and CD8 expression. Numbers indicate the percentages of cells in each gate. (C) Vβ10b and Vα11.1/.2 expression after gating on CD4^{+} thymocytes or CD4^{+} splenocytes from the indicated mice. Shaded gray histograms represent CD4^{+} T cells from B6 mice; continuous lines represents CD4^{+} T cells from C7 TCR tg mice. Black and small gray numbers indicate the percentages of stained cells among CD4^{+} T cells from C7 TCR tg or B6 mice, respectively. (D) Purified CD4^{+} T cells from C7 TCR tg or B6 mice were stimulated with ESAT-6 peptide in the presence of APCs. Proliferation was measured by [^{3}H]thymidine incorporation between 48 and 72 h of culture. Error bars in A and D represent SDs.

C7 Th1 effector cells protect mice from infection

Mice immunized with *M. tuberculosis* proteins plus adjuvant, BCG variants, or *M. tuberculosis* are, in comparison to naive controls, protected from challenge with *M. tuberculosis*. These immunization protocols induce complex populations of *M. tuberculosis*–specific CD4^{+} and CD8^{+} T cells that contribute to protection. The CD4^{+} T cell populations are mixed and may include Th1, Th17, and suppressive regulatory T cell populations (14–16). In one report, in vitro–generated monoclonal Th1 cells (specific to ovalbumin) were shown to provide ∼1 log of protection in animals infected with *M. tuberculosis* expressing the model antigen ovalbumin (29).

Because ESAT-6 is a native *M. tuberculosis* antigen and a target for vaccine development (30), we wanted to understand if a pure population of ESAT-6–specific C7 Th1 cells could protect mice from infection. B6 hosts received 10[7] in vitro–generated C7 Th1 cells (or control Th1 cells) and were then infected with 100 CFU *M. tuberculosis* 1 d later. Before transfer, the differentiation status of the cells was verified by analysis of CD44 and T-bet expression (Fig. 4 A). 24 d after infection, the number of bacteria in the lungs was determined. Surprisingly,

C7 Th1 cells decreased the number of viable bacteria by a factor of 100, whereas animals that received control Th1 cells contained similar numbers of bacteria as mice that received no cells (Fig. 4 B). Next, we sought to determine if fewer C7 Th1 cells could protect animals from *M. tuberculosis* challenge. Graded numbers of C7 Th1 cells (10[5], 10[6], or 10[7]) were transferred into B6 recipients, and bacterial numbers were determined 16, 30, and 90 d after infection. These results show that the degree of protection correlates with the dose of C7 Th1 cells transferred. Administration of as few as 10[5] cells was sufficient to provide significant protection that was sustained for up to 90 d after infection (Fig. 4, C and D). Interestingly, although the day 30 numbers of bacteria were maintained until day 90 after infection in animals that received low doses of cells, bacterial numbers increased in animals that received 10[7] C7 Th1 cells (Fig. 4 D).

These studies demonstrate that ESAT-6–specific Th1 cells can greatly reduce the numbers of *M. tuberculosis* in the lungs. Compared with control mice, animals that received 10[7] C7 Th1 cells had a 99% reduction in the number of viable bacteria early after infection.
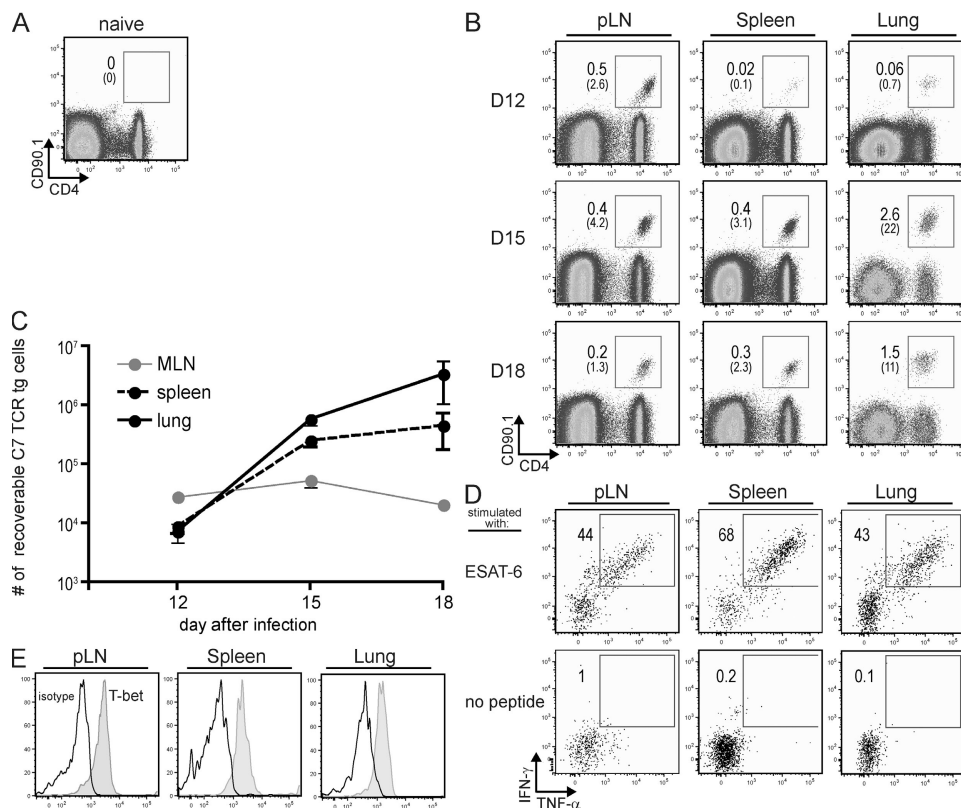

Figure 2. C7 TCR tg CD4^{+} T cells respond to *M. tuberculosis* infection in vivo. (A) 10[4] C7 TCR tg.RAG^{−/−} CD4^{+} T cells (CD90.1) were transferred into uninfected congenically marked B6 recipients (CD90.2), and splenocytes were stained for CD4 and CD90.1 expression 7 d later. The gate marks donor-derived C7 TCR tg.RAG^{−/−} CD4^{+} T cells (CD90.1^{+}) cells, and the percentages of these cells within total cells (top) or among CD4^{+} T cells (bottom) are shown. (B–E) As in A, except mice were aerosol infected 1 d after T cell transfer with 100 CFU *M. tuberculosis*. pLNs, spleen, and lung were examined 12, 15, and 18 d later. (C) Graphic representation of results from three to four mice per time point. Error bars represent SDs. (D) C7 TCR tg.RAG^{−/−} CD4^{+} T cells from the indicated organs were harvested from day 15–infected mice, and their ability to make IFN-γ and TNF-α was determined after stimulation with ESAT-6 peptide or medium alone. (E) Intracellular T-bet (shaded histogram) or isotype control staining (continuous line) of C7 TCR tg.RAG^{−/−} CD4^{+} T cells taken from the indicated organs 15 d after infection. The data presented in this figure are representative of two experiments with three to four mice per group.

C7 Th1 cells control bacterial replication after 1 wk following infection

Use of C7 TCR tg cells in the previous experiments demonstrated that naive ESAT-6–specific CD4+ T cells were primed in the pLNs between 7 and 10 d after infection, and these cells differentiated into Th1 effector cells and trafficked to the lungs between 12 and 14 d after infection (Figs. 2 and 3). These observations are consistent with other studies that have measured endogenous T cell responses to *M. tuberculosis* and demonstrated that antigen-specific T cell responses were detected in the pLNs 14 d after infection, and reached peak numbers in the lungs ~28 d after infection, at which time in vivo bacterial growth was controlled (24–26).

Our experiments with in vitro–generated C7 Th1 cells demonstrated that these cells greatly reduced the bacterial numbers in the lungs as early as day 16 after infection. In the ensuing experiments, we wanted to look earlier than day 16 after infection to determine when C7 Th1 cells manifest protection. 10^7 C7 Th1 cells were transferred into mice that were infected 1 d later with *M. tuberculosis*, and bacterial numbers in the lungs were determined early after infection. Before infection, ~5 × 10^5 C7 Th1 cells were recovered from either spleen or lungs, and these cells were functional, producing both IFN-γ and TNF-α after ex vivo stimulation (Fig. 5, A–C).

To our surprise, despite the high numbers of C7 effector cells in the lungs, similar numbers of bacteria were recovered from animals that received C7 Th1 cells and from control animals during the first 7 d of infection. In contrast, between days 7 and 10 after infection, while bacterial growth continued in control mice, growth was controlled in animals that received C7 Th1 cells. Interestingly, the number of bacteria remained constant until day 30 after infection despite the presence of C7 Th1 cells capable of producing cytokines in the lungs (Fig. 5, D and E).

The finding that C7 Th1 cells were in the lungs before infection, but did not control bacterial replication until after day 7 following infection, led us to investigate whether these cells were activated during the first week of infection. Unlike our studies using naive C7 cells, we could not determine, using the activation markers CD69 and CD25, when C7 Th1 effector cells were presented antigen in the lung, because ~60% of C7 Th1 cells expressed these activation markers regardless of whether these cells were harvested from naive or infected animals (Fig. S1, available at http://www.jem.org/cgi/content/full/jem.20080353/DC1). This result is consistent with studies of memory CD8 T cells in the lung and suggests that CD69 cannot be used to monitor presentation of cognate antigen to antigen-experienced T cells in the lung (31). In addition, expansion of C7 Th1 cells was not evident in infected animals between days 4 and 13 after infection, because similar numbers of C7 Th1 cells were recovered from naive and infected mice (Fig. S1). As a third attempt to understand if C7 Th1 cells were activated during the first 7 d of infection, message levels for *ifnγ* and one target gene, *nos2*, were measured in infected mice that received C7 Th1 cells. Similar levels of these transcripts were observed from days 1

to 7 after infection, whereas both transcripts were induced by day 18 after infection. This suggests that C7 Th1 cells were not activated to produce high levels of IFN-γ during the first week of infection. Collectively, these data do not support the hypothesis that C7 Th1 cells are activated during the first 7 d of infection. However, these negative data also do not rule out the possibility that some C7 Th1 cells (perhaps very small numbers) "see" antigen and are activated during the first week of infection.
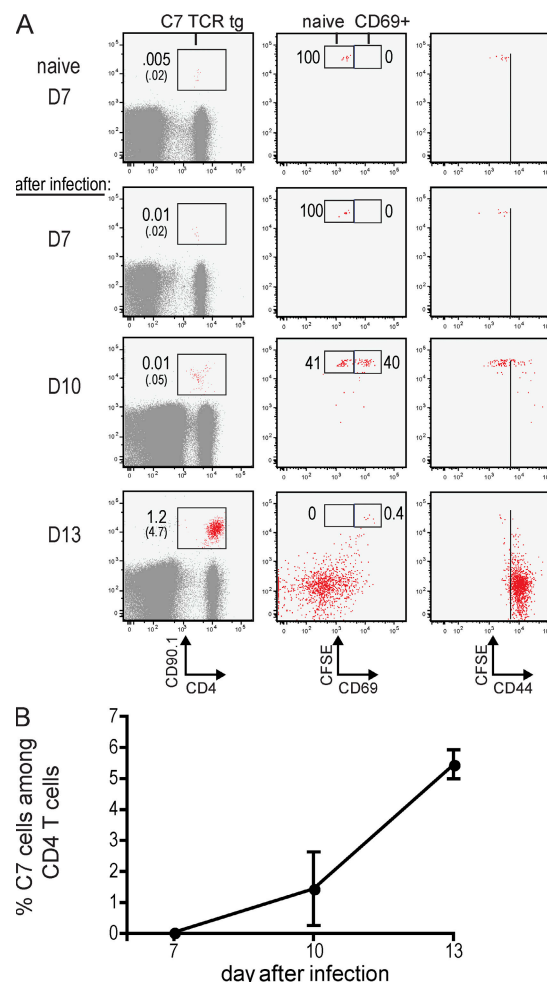

Figure 3. Naive C7 TCR tg CD4+ T cells are activated in the pLNs between days 7 and 10 after infection. (A) 10^5 CFSE-labeled C7 TCR tg.RAG$^{-/-}$ CD4+ T cells (CD90.1) were transferred into congenically marked B6 recipients (CD90.2) that were left uninfected (top row, naive) or aerosol infected with 100 CFU *M. tuberculosis* 1 d later (bottom three rows, after infection). The first column shows CD4 and CD90.1 staining of pLN cells. Gate marks donor-derived C7 TCR tg.RAG$^{-/-}$ CD4+ T cells (CD90.1+), and the percentage of these cells within total pLNs (top) or among CD4+ T cells (bottom) is shown. The second and third columns show CFSE intensity and CD69 staining or CD44 staining, respectively, on gated C7 TCR tg.RAG$^{-/-}$ CD4+ T cells. Numbers indicate the percentages of cells in the indicated gates. (B) Graphic representation of results from three to four mice per time point for the experiment described in A. Error bars represent SDs. The data presented in this figure are representative of three experiments of similar design with two to four mice per group.

In summary, the results show that effector ESAT-6–specific Th1 cells greatly reduce the number of viable *M. tuberculosis* in the lungs and that control of bacterial growth occurs after day 7 following infection. This delay in protection is unlikely to be caused by a lack of ESAT-6 synthesis during the first week of infection, because ESAT-6 transcript was detectable by at least day 5 after infection in the lungs of infected mice, and ESAT-6–deficient *M. tuberculosis* showed reduced growth in the lungs (compared with wild-type *M. tuberculosis*) during the first 5 d of infection, demonstrating that ESAT-6 is synthesized very early after infection (32, 33).

DISCUSSION

We generated mice tg for a TCR specific to the dominant *M. tuberculosis* antigen ESAT-6 to investigate the ability of Th1 cells to provide protective immunity. Our analysis of adoptively transferred C7 TCR tg CD4+ T cells revealed that priming of naive ESAT-6–specific TCR tg cells occurred 7–10 d after aerosol infection with a low dose of *M. tuberculosis*. Our experiments demonstrated that adoptively transferred Th1 cells specific for ESAT-6 can provide a high level of protection, as measured up to 90 d after infection, but that in vivo mycobac-

terial growth is unimpaired for the first week of infection despite large numbers of pathogen-specific T cells in the lungs.

The delay in priming of naive ESAT-6–specific T cells is not unexpected and is consistent with the finding that *M. tuberculosis*–specific effector T cells are not present at high frequencies in the lungs of mice until ∼3 wk after infection (24, 25). Our results are also consistent with a recent study (34) that monitored the priming of TCR tg CD4+ T cells specific to the *M. tuberculosis* antigen Ag85B. One notable difference is that priming of Ag85B-specific monoclonal CD4+ T cells occurred at day 12 after aerosol infection, 2–4 d later than the C7 TCR tg cell response documented in this study. Differences in priming between naive Ag85B and ESAT-6–specific clones may result from differences in the expression patterns of these two proteins (32), differences in the presentation of these antigens, or differences in the sensitivity of the TCRs used by Ag85B TCR tg cells and C7 TCR tg cells for their cognate antigens. Direct comparative studies will be required to distinguish between these possibilities.

Our studies with in vitro–generated Th1 cells revealed two surprising findings. One is how well monoclonal ESAT-6–specific Th1 cells were able to protect mice from *M. tuberculosis*
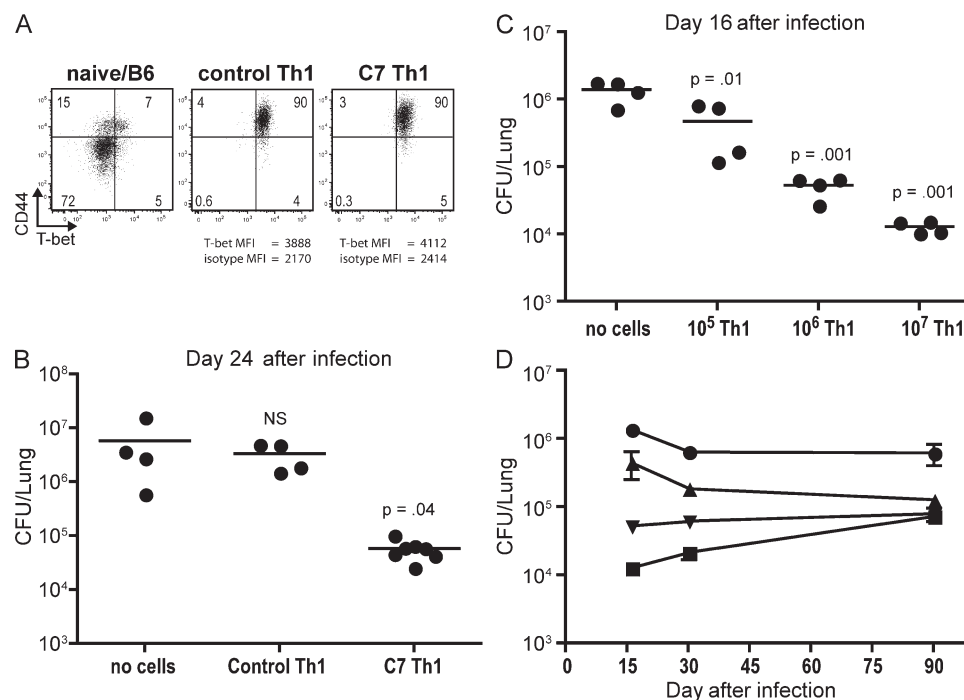
Figure 4. Adoptive transfer of C7 Th1 T cells confers protection to *M. tuberculosis*. (A) B6 or C7 CD4+ T cells were stimulated in vitro with anti-CD3/CD28 (control Th1 cells) or ESAT-6 peptide (C7 Th1 cells), respectively, in the presence of IFN-γ and anti–IL-4 for 4 d, and were analyzed for CD44 and T-bet expression. CD4+ T cells from naive B6 spleens are shown as a staining control. Numbers represent the percentages of cells in each quadrant. MFI, mean fluorescence intensity. (B) 10^7 Th1-differentiated B6 or C7 CD4+ T cells were transferred into B6 recipient mice 1 d before aerosol infection with 100 CFU *M. tuberculosis*. 24 d later, the number of bacteria in the lungs was determined. Each symbol represents data from one mouse, and p-values compare the CFU from mice that received no cells compared with mice that received either B6 or C7 Th1 cells. The experiment was performed two times with similar results. Horizontal bars represent the mean. (C and D) Similar experiment as in B, except 10^7, 10^6, or 10^5 C7 Th1 cells or no cells were transferred and CFU were determined 16, 30, and 90 d after infection. This experiment was preformed one time with four mice per group. In C, each circle represents data from one mouse, and p-values compare the CFU from mice that received no cells. In D, each symbol represents four mice per group (square, 10^7 cells; inverted triangle, 10^6 cells; triangle, 10^5 cells; and circle, no cells). Error bars represent SDs.

infection. The second is the fact that despite high numbers of C7 Th1 effector cells in animals before infection, bacterial replication was not controlled until 1 wk after infection.

The 2-log reduction in the number of bacilli in animals that received C7 Th1 cells is greater than that observed after BCG immunization and comparable to prime-boost vaccina-

tion methods (35, 36). By using adoptively transferred C7 Th1 cells, our experiments demonstrate that monoclonal T cells specific to ESAT-6 can provide a level of early protection that is comparable to that provided by mixed populations of *M. tuberculosis*–specific CD4^{+} and CD8^{+} effector T cells after vaccination. Thus, complex populations of T cells
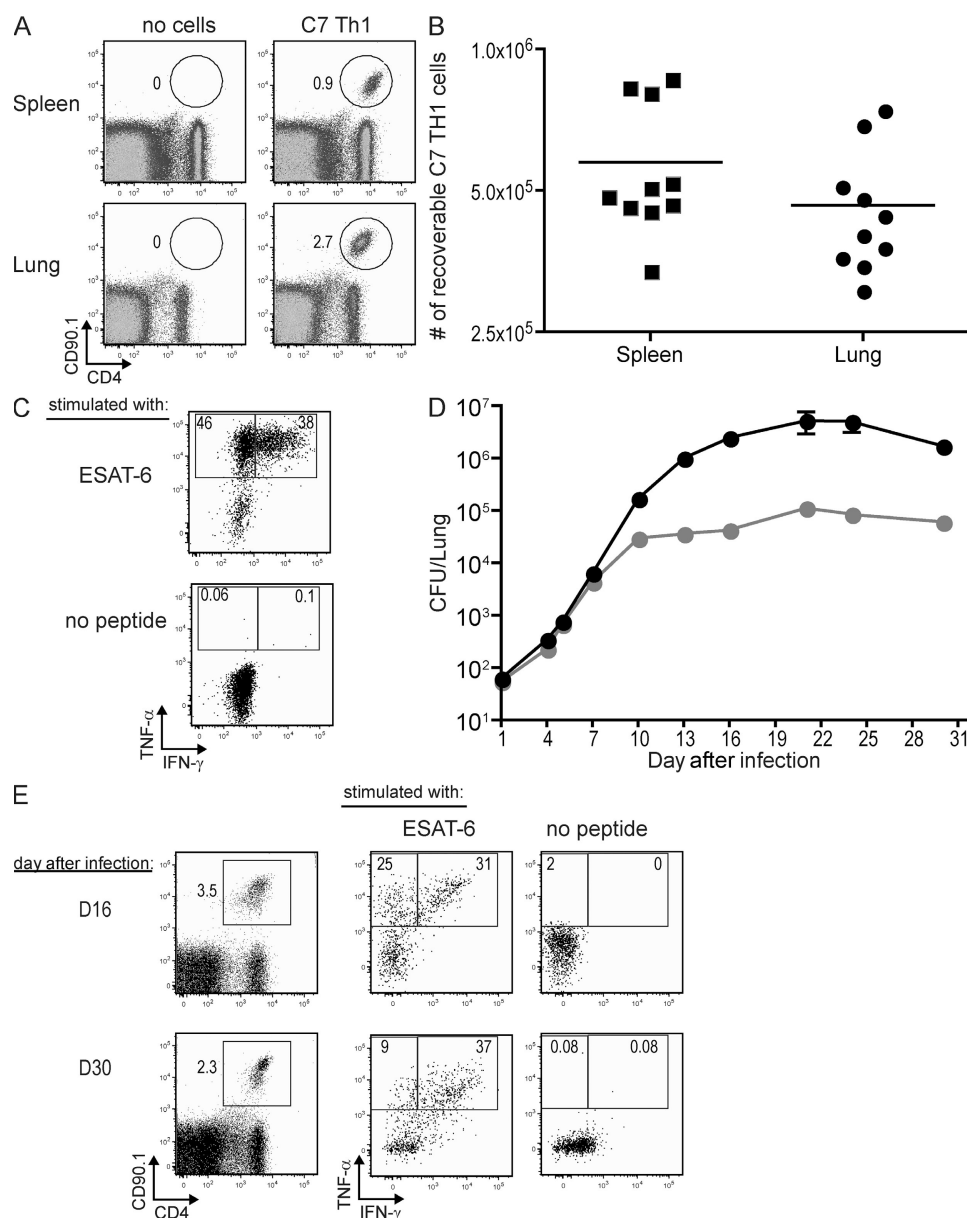

Figure 5.   C7 Th1 cells confer protection to *M. tuberculosis* only after day 7 following infection. (A–C) 10[7] C7 Th1 cells (CD90.1) were transferred into B6 recipient mice (CD90.2), and 1 d later splenocytes or lung cells were harvested and stained for CD4 and CD90.1 expression. (A) Gate marks donor-derived cells among total cells in the indicated organs. (B) Graphic representation showing the number of recoverable C7 Th1 cells from the indicated organs. Each symbol represents data from one mouse. (C) Intracellular TNF-α and IFN-γ staining of C7 Th1 cells harvested from the lungs. bars in B and C represent the mean. (D) Similar experiment as in A–C, except mice were infected 1 d after T cell transfer with 100 CFU *M. tuberculosis*. Bacterial numbers were determined at the indicated days after infection. The data presented is a compilation of five experiments. Each time point includes CFU data from 7–12 mice per time point with the exception of days 4 and 5, which have 4 mice per time point. Error bars represent SDs. (E) Lung cells were harvested from day 16– or day 30–infected mice and were stained for CD4 and CD90.1 expression (left). Gate marks donor-derived cells among total cells. Intracellular TNF-α and IFN-γ staining of C7 Th1 cells harvested from the lungs is shown (right).

are not required to control infection, a result that suggests that adoptive T cell transfer may provide a therapeutic option for drug-resistant *M. tuberculosis* infections.

It is presumed that improved vaccines can be designed to protect individuals from *M. tuberculosis* infection by eliciting robust antigen-specific T cell responses. This view is supported by the observation that after aerosol infection in mice, accumulation of *M. tuberculosis* CD4+ T cells in the lungs coincides with the control of bacterial growth (6, 14, 37). Several hypotheses for a lack of sterilizing immunity to *M. tuberculosis* can be proposed, including a delayed recruitment of effector T cells to the lungs. Our ability to track adoptively transferred *M. tuberculosis*–specific C7 Th1 cells allowed us to determine that approximately a half million of these cells were in the lungs before infection and allowed us to definitively rule out this hypothesis.

What accounts for the delayed protection by C7 Th1 cells? Given the low dose infection used in our studies (100 bacteria) and the slow doubling time of *M. tuberculosis* during the first several days of infection, very few cells may be infected, and the probability of C7 Th1 cells "finding" an infected cell may be low. Although several cell types, including macrophages and DCs, are infected by day 14 after infection (38), no information exists on the frequency or phenotype of infected cells in the lungs during the first week of infection (although presumably alveolar macrophages are the first cells infected). A recent study using multiphoton microscopy found that liver-resident macrophages, Kupffer cells, were the first cells infected with BCG after i.v. infection (39). Recruitment of uninfected Kupffer cells and blood-derived monocytes to infected cells occurred 2 wk after infection.

If similar delays in cell recruitment occur in the lungs after *M. tuberculosis* infection, it could take 7–10 d until lung resident cells (i.e., macrophages, DCs, and effector/memory T cells) home to infected cells. Before day 7 after infection, C7 Th1 cells may randomly encounter infected cells, whereas after day 7, migration within the lungs to infected sites could be directed by inflammatory signals. Our studies with naive C7 CD4+ T cells demonstrated that T cell priming in pLNs also occurred only after day 7 following infection. A similar mechanism may account for the delayed priming of naive CD4+ T cells. After the first week of infection, DCs and other APCs may home to infected sites within the lung and traffic to draining LNs to prime naive T cells. This hypothesis requires further investigation.

On the other hand, if C7 Th1 cells home to infected cells within the lungs promptly after infection, it would suggest defective collaboration between CD4+ effector cells and infected cells: infected cells may be unable to present antigen to activate effector CD4+ T cells, or infected cells may be unable to control bacterial replication after stimulation by IFN-γ and other factors provided by effector CD4+ T cells. In vitro studies support both hypotheses, but in vivo studies to answer these important questions are necessary (40–45).

The findings reported in this paper have important implications for understanding immunity to *M. tuberculosis*. In this study, we show that high numbers of ESAT-6–specific Th1 cells provided substantial protection to mice after low dose aerosol infection with *M. tuberculosis*. However, this protection was delayed until after day 7 following infection, and bacteria persisted in these animals thereafter. This finding may help explain why vaccination against *M. tuberculosis* has been difficult: immediately after infection, *M. tuberculosis* resides in cells that CD4+ T cells cannot help.

MATERIALS AND METHODS

Generation of C7 TCR tg mice. To generate ESAT-6–specific CD4+ T cell hybridomas, B6 mice were aerosol infected with ∼100 CFU *M. tuberculosis* Erdman, and 6 wk after infection, CD4+ splenocytes were purified and stimulated in the presence of irradiated T cell–depleted splenocytes (APCs) and 0.5 μg/ml of ESAT-6 protein (the expression vector used to make ESAT-6 protein, pMRLB7, was provided by Mycobacteria Research Laboratories at Colorado State University). 2 d later, activated CD4+ T cells were fused with the tumor cell line BW5147. Antigen-specific CD4+ T cell hybridomas were selected by screening for IL-2 production in response to ESAT-6 protein and ESAT-6$_{1-20}$ peptide. TCR chains were identified by a combination of surface staining with a panel of TCR Vα and Vβ chain monoclonal antibodies (BD Biosciences), and by RT-PCR amplification and DNA sequencing. Hybridoma clone 7 was chosen to generate TCR tg mice because it expressed only one in-frame TCR α chain, and monoclonal antibodies were available for both TCR chains. The TCR chains conferring the specificity of clone 7 hybridoma cells were identified as Vβ10b-Dβ1.1-Jβ2.4 and Vα11.2-Jα27. TCR α chain variable region (VJ) and β chain variable region (VDJ) cDNAS were amplified with the following primers: Vβ10b-Dβ1.1-Jβ2.4, (5′ primer) 5′-tgctgccctcgaggatcgacgaattcacaggggccatgcagaggaa-3′ and (3′ primer) 5′-agcaggttccggattctggatgtttgg-3′; and Vα11.2-Jα27, (5′ primer) 5′-tgctgccctcgaggatcgacgaattcgacccaactatgggctgta-3′ and (3′ primer) 5′-tttct-cagatcttctagcaccgatagtcgg-3′.

VJ and VDJ cDNAS were subcloned into pBluescript vectors that contained TCR α or β chain constant regions. Complete TCR α and β chains were excised and cloned into the VA hCD2 vectors (pBluescript and VA hCD2 were provided by E. Huesby, University of Massachusetts Medical School, Worcester, MA) (23). DNA fragments containing the TCR cDNAs were injected into fertilized B6 oocysts. Founders and their progeny were screened by flow cytometry for surface expression of Vβ10b and Vα11.1/.2. TCR tg founder number 27 was selected and used in all experiments presented in this paper.

Mice and adoptive cell transfers. B6 mice were purchased from the Jackson Laboratory. All animal procedures were approved by the Memorial Sloan-Kettering Institutional Animal Care and Use Committee. C7 TCR tg mice were bred to B6.CD90.1 mice to obtain C7 TCR tg.CD90.1 mice, and to RAG$^{-/-}$.CD90.1 mice to generate C7 TCR tg.RAG$^{-/-}$.CD90.1 mice. C7 TCR tg mice were maintained at the animal facility in the Memorial Sloan-Kettering Research Animal Resource Center. For adoptive transfer experiments, C7 TCR tg CD4+ T cells were isolated from the spleen and LNs of TCR tg mice. Cells were injected i.v. into naive recipients 1 d before infection. In some experiments cells were labeled with 5 μM CFSE before transfer.

Generation of Th1 cells. 3×10^6 purified C7 TCR tg CD4+ T cells were cultured with 12×10^6 irradiated T cell–depleted splenocytes. 5 μg/ml of ESAT-6$_{1-20}$ peptide, 10 ng/ml IL-12, and 5 μg/ml of neutralizing anti–IL-4 antibody (R&D Systems) were added at day 0 of culture. At days 2 and 3 of culture, the cells were split 1:2, and 50 U/ml IL-2 was added (R&D Systems). On day 4 of culture, Th1 cell differentiation was confirmed via intracellular expression of T-bet. The same protocol was used to make polyclonal Th1 CD4+ T cells, except the CD4+ T cells were taken from B6 mice and stimulated in the presence of 1 μg/ml anti-CD3 (145-2C11) and 0.5 μg/ml anti-CD28 (37.51). Th1 cells were washed three times with PBS and injected i.v. into B6 mice.

In vitro T cell proliferation and IL-2 production. 5×10^4 clone 7 hybridoma cells, BW5147 cells, or purified $CD4^+$ T cells harvested from B6 or C7 TCR tg mice were plated with 1.5×10^5 irradiated T cell–depleted splenocytes in 96-well round-bottom plates in the presence of various concentrations of ESAT-6_{1-20} peptide. For proliferation experiments, cells were pulsed between days 2 and 3 of culture by the addition of 1 μCi [^{3}H]thymidine per well for 16 h before harvesting cells onto glass-fiber filters and determining the incorporated radioactivity using a liquid scintillation counter (TopCount; PerkinElmer). For IL-2 ELISAs, supernatants were harvested after 2 d of stimulation, and IL-2 levels were measured with a mouse IL-2 ELISA set (BD Biosciences).

Intracellular staining. To detect intracellular cytokines 3×10^6 cells from pLNs, spleen, or collagenase-digested and –perfused lungs were plated in 96-well round-bottom plates in the presence of GolgiPlug (BD Biosciences) and 5 μg/ml ESAT-6_{1-20} peptide. 5 h later, cells were washed and stained with cell-surface antibodies, and intracellular cytokine (ICC) staining was performed according to the manufacturer's instructions. Cells harvested from *M. tuberculosis*–infected mice were fixed with 2% paraformaldehyde overnight before removal from the biosafety level 3 facility. These cells were washed and permeabilized, and ICC staining was performed. Intracellular T-bet and isotype control staining (anti–T-bet–PE 4B10 [Santa Cruz Biotechnology, Inc.] and mouse IgG1-PE [BD Biosciences]) were performed using reagents supplied with the mouse regulatory T cell staining kit (eBioscience).

Aerosol infections with *M. tuberculosis*. *M. tuberculosis* Erdman was grown in 7H9 media, and log-phase cultures were diluted to 8×10^6 *M. tuberculosis* per millimeter and were sonicated before infection with an aerosol exposure system (Glass-Col). 8–10-wk-old B6 mice were infected with a volume of suspension, and exposure time was calibrated to deliver $\sim$100 CFU per animal. To determine the infection dose, three mice were killed 1 d after infection and lungs were harvested and homogenized in PBS/0.05% Tween-80, and half of the lung homogenate was plated. At various time intervals after infection, the right lung was harvested from individual mice and homogenized in PBS/0.05% Tween-80. Serial dilutions were made in PBS/0.05% Tween-80 and plated onto Middlebrook 7H10 agar (BD Biosciences). After 3–4 wk of incubation at 37°C in a 5% CO_2 atmosphere, mycobacterial colonies were counted and the bacterial numbers in the lungs were calculated.

Real-time PCR analysis. Total RNA was isolated from lung parenchyma using TRIzol reagent (Invitrogen), and cDNA was synthesized from DNase-treated RNA using oligo(dT) primers and SuperScript II (Invitrogen). RNA was pooled from four mice per group. SYBR green–based real-time PCR analysis was performed using the DynNAmo SYBR green qPCR kit (Finnzymes). *ifnγ* and *nos2* primers were purchased from QIAGEN. Signals were normalized to GAPDH transcript (forward, 5′-ACCACAGTCCATGCCATCAC-3′; reverse, 5′-TCCACCACCCTGTTGCTGTA-3′). To determine levels of *ifnγ* and *nos2*, the following equation was used, where n equals the difference in PCR cycle number between *ifnγ* and GAPDH at which the signals were first detected above background (Ct): $1/2^{n = \text{Ct } ifn\gamma - \text{Ct GAPDH}}$.

Statistical analysis. Statistical analysis was performed with the unpaired Student's *t* test on Prism software. $P \leq 0.05$ was considered significant. Error bars denote SDs.

Online supplemental material. Fig. S1 A shows CD69 and CD25 expression on gated C7 Th1 cells harvested from the lungs of naive and infected mice. Fig. S1 B shows numbers of recoverable C7 Th1 cells from infected mice. Fig. S1 C depicts a real-time PCR analysis of *ifnγ* and *nos2* transcripts from the lungs of infected mice. Online supplemental material is available at http://www.jem.org/cgi/content/full/jem.20080353/DC1.

REFERENCES

1. Keane, J., S. Gershon, R.P. Wise, E. Mirabile-Levens, J. Kasznica, W.D. Schwieterman, J.N. Siegel, and M.M. Braun. 2001. Tuberculosis associated with infliximab, a tumor necrosis factor alpha–neutralizing agent. *N. Engl. J. Med.* 345:1098–1104.

2. Cooper, A.M., D.K. Dalton, T.A. Stewart, J.P. Griffin, D.G. Russell, and I.M. Orme. 1993. Disseminated tuberculosis in interferon γ gene-disrupted mice. *J. Exp. Med.* 178:2243–2247.

3. Flynn, J.L., J. Chan, K.J. Triebold, D.K. Dalton, T.A. Stewart, and B.R. Bloom. 1993. An essential role for interferon γ in resistance to *Mycobacterium tuberculosis* infection. *J. Exp. Med.* 178:2249–2254.

4. van de Vosse, E., M.A. Hoeve, and T.H. Ottenhoff. 2004. Human genetics of intracellular infectious diseases: molecular and cellular immunity against mycobacteria and salmonellae. *Lancet Infect. Dis.* 4:739–749.

5. Flynn, J.L., M.M. Goldstein, J. Chan, K.J. Triebold, K. Pfeffer, C.J. Lowenstein, R. Schreiber, T.W. Mak, and B.R. Bloom. 1995. Tumor necrosis factor-alpha is required in the protective immune response against *Mycobacterium tuberculosis* in mice. *Immunity.* 2:561–572.

6. North, R.J., and Y.J. Jung. 2004. Immunity to tuberculosis. *Annu. Rev. Immunol.* 22:599–623.

7. van Rie, A., R. Warren, M. Richardson, T.C. Victor, R.P. Gie, D.A. Enarson, N. Beyers, and P.D. van Helden. 1999. Exogenous reinfection as a cause of recurrent tuberculosis after curative treatment. *N. Engl. J. Med.* 341:1174–1179.

8. Caminero, J.A., M.J. Pena, M.I. Campos-Herrero, J.C. Rodriguez, O. Afonso, C. Martin, J.M. Pavon, M.J. Torres, M. Burgos, P. Cabrera, et al. 2001. Exogenous reinfection with tuberculosis on a European island with a moderate incidence of disease. *Am. J. Respir. Crit. Care Med.* 163:717–720.

9. Andersen, P., and T.M. Doherty. 2005. The success and failure of BCG - implications for a novel tuberculosis vaccine. *Nat. Rev. Microbiol.* 3: 656–662.

10. Mogues, T., M.E. Goodrich, L. Ryan, R. LaCourse, and R.J. North. 2001. The relative importance of T cell subsets in immunity and immunopathology of airborne *Mycobacterium tuberculosis* infection in mice. *J. Exp. Med.* 193:271–280.

11. Caruso, A.M., N. Serbina, E. Klein, K. Triebold, B.R. Bloom, and J.L. Flynn. 1999. Mice deficient in CD4 T cells have only transiently diminished levels of IFN-gamma, yet succumb to tuberculosis. *J. Immunol.* 162:5407–5416.

12. Tascon, R.E., E. Stavropoulos, K.V. Lukacs, and M.J. Colston. 1998. Protection against *Mycobacterium tuberculosis* infection by CD8+ T cells requires the production of gamma interferon. *Infect. Immun.* 66:830–834.

13. Markowitz, N., N.I. Hansen, P.C. Hopewell, J. Glassroth, P.A. Kvale, B.T. Mangura, T.C. Wilcosky, J.M. Wallace, M.J. Rosen, and L.B. Reichman. 1997. Incidence of tuberculosis in the United States among HIV-infected persons. The Pulmonary Complications of HIV Infection Study Group. *Ann. Intern. Med.* 126:123–132.

14. Khader, S.A., G.K. Bell, J.E. Pearl, J.J. Fountain, J. Rangel-Moreno, G.E. Cilley, F. Shen, S.M. Eaton, S.L. Gaffen, S.L. Swain, et al. 2007. IL-23 and IL-17 in the establishment of protective pulmonary CD4+ T cell responses after vaccination and during *Mycobacterium tuberculosis* challenge. *Nat. Immunol.* 8:369–377.

15. Scott-Browne, J.P., S. Shafiani, G. Tucker-Heard, K. Ishida-Tsubota, J.D. Fontenot, A.Y. Rudensky, M.J. Bevan, and K.B. Urdahl. 2007. Expansion and function of Foxp3-expressing T regulatory cells during tuberculosis. *J. Exp. Med.* 204:2159–2169.

16. Kursar, M., M. Koch, H.W. Mittrucker, G. Nouailles, K. Bonhagen, T. Kamradt, and S.H. Kaufmann. 2007. Cutting Edge: Regulatory T cells prevent efficient clearance of *Mycobacterium tuberculosis*. *J. Immunol.* 178:2661–2665.

17. Pym, A.S., P. Brodin, R. Brosch, M. Huerre, and S.T. Cole. 2002. Loss of RD1 contributed to the attenuation of the live tuberculosis vaccines *Mycobacterium bovis* BCG and *Mycobacterium microti*. *Mol. Microbiol.* 46:709–717.

18. Brandt, L., T. Oettinger, A. Holm, A.B. Andersen, and P. Andersen. 1996. Key epitopes on the ESAT-6 antigen recognized in mice during the recall of protective immunity to *Mycobacterium tuberculosis*. *J. Immunol.* 157:3527–3533.

19. Ulrichs, T., M.E. Munk, H. Mollenkopf, S. Behr-Perst, R. Colangeli, M.L. Gennaro, and S.H. Kaufmann. 1998. Differential T cell responses to *Mycobacterium tuberculosis* ESAT6 in tuberculosis patients and healthy donors. *Eur. J. Immunol.* 28:3949–3958.

20. Sorensen, A.L., S. Nagai, G. Houen, P. Andersen, and A.B. Andersen. 1995. Purification and characterization of a low-molecular-mass T-cell antigen secreted by *Mycobacterium tuberculosis*. *Infect. Immun.* 63:1710–1717.

21. Lin, P.L., S. Pawar, A. Myers, A. Pegu, C. Fuhrman, T.A. Reinhart, S.V. Capuano, E. Klein, and J.L. Flynn. 2006. Early events in *Mycobacterium tuberculosis* infection in cynomolgus macaques. *Infect. Immun.* 74:3790–3803.

22. Weinrich Olsen, A., L.A. van Pinxteren, L. Meng Okkels, P. Birk Rasmussen, and P. Andersen. 2001. Protection of mice with a tuberculosis subunit vaccine based on a fusion protein of antigen 85b and esat-6. *Infect. Immun.* 69:2773–2778.

23. Zhumabekov, T., P. Corbella, M. Tolaini, and D. Kioussis. 1995. Improved version of a human CD2 minigene based vector for T cell-specific expression in transgenic mice. *J. Immunol. Methods.* 185:133–140.

24. Winslow, G.M., A.D. Roberts, M.A. Blackman, and D.L. Woodland. 2003. Persistence and turnover of antigen-specific CD4 T cells during chronic tuberculosis infection in the mouse. *J. Immunol.* 170:2046–2052.

25. Lazarevic, V., D. Nolt, and J.L. Flynn. 2005. Long-term control of *Mycobacterium tuberculosis* infection is mediated by dynamic immune responses. *J. Immunol.* 175:1107–1117.

26. Chackerian, A.A., J.M. Alt, T.V. Perera, C.C. Dascher, and S.M. Behar. 2002. Dissemination of *Mycobacterium tuberculosis* is influenced by host factors and precedes the initiation of T-cell immunity. *Infect. Immun.* 70:4501–4509.

27. Rivera, A., G. Ro, H.L. Van Epps, T. Simpson, I. Leiner, D.B. Sant'Angelo, and E.G. Pamer. 2006. Innate immune activation and CD4+ T cell priming during respiratory fungal infection. *Immunity.* 25:665–675.

28. Roman, E., E. Miller, A. Harmsen, J. Wiley, U.H. Von Andrian, G. Huston, and S.L. Swain. 2002. CD4 effector T cell subsets in the response to influenza: heterogeneity, migration, and function. *J. Exp. Med.* 196:957–968.

29. Wangoo, A., T. Sparer, I.N. Brown, V.A. Snewin, R. Janssen, J. Thole, H.T. Cook, R.J. Shaw, and D.B. Young. 2001. Contribution of Th1 and Th2 cells to protection and pathology in experimental models of granulomatous lung disease. *J. Immunol.* 166:3432–3439.

30. Brodin, P., I. Rosenkrands, P. Andersen, S.T. Cole, and R. Brosch. 2004. ESAT-6 proteins: protective antigens and virulence factors? *Trends Microbiol.* 12:500–508.

31. Kohlmeier, J.E., S.C. Miller, and D.L. Woodland. 2007. Cutting edge: Antigen is not required for the activation and maintenance of virus-specific memory CD8+ T cells in the lung airways. *J. Immunol.* 178:4721–4725.

32. Rogerson, B.J., Y.J. Jung, R. LaCourse, L. Ryan, N. Enright, and R.J. North. 2006. Expression levels of *Mycobacterium tuberculosis* antigen-encoding genes versus production levels of antigen-specific T cells during stationary level lung infection in mice. *Immunology.* 118:195–201.

33. Stanley, S.A., S. Raghavan, W.W. Hwang, and J.S. Cox. 2003. Acute infection and macrophage subversion by *Mycobacterium tuberculosis* require a specialized secretion system. *Proc. Natl. Acad. Sci. USA.* 100:13001–13006.

34. Wolf, A.J., L. Desvignes, B. Linas, N. Banaiee, T. Tamura, K. Takatsu, and J.D. Ernst. 2008. Initiation of the adaptive immune response to *Mycobacterium tuberculosis* depends on antigen production in the local lymph node, not the lungs. *J. Exp. Med.* 205:105–115.

35. Grode, L., P. Seiler, S. Baumann, J. Hess, V. Brinkmann, A. Nasser Eddine, P. Mann, C. Goosmann, S. Bandermann, D. Smith, et al. 2005. Increased vaccine efficacy against tuberculosis of recombinant *Mycobacterium bovis* bacille Calmette-Guerin mutants that secrete listeriolysin. *J. Clin. Invest.* 115:2472–2479.

36. Goonetilleke, N.P., H. McShane, C.M. Hannan, R.J. Anderson, R.H. Brookes, and A.V. Hill. 2003. Enhanced immunogenicity and protective efficacy against *Mycobacterium tuberculosis* of bacille Calmette-Guerin vaccine using mucosal administration and boosting with a recombinant modified vaccinia virus Ankara. *J. Immunol.* 171:1602–1609.

37. Jung, Y.J., L. Ryan, R. LaCourse, and R.J. North. 2005. Properties and protective value of the secondary versus primary T helper type 1 response to airborne *Mycobacterium tuberculosis* infection in mice. *J. Exp. Med.* 201:1915–1924.

38. Wolf, A.J., B. Linas, G.J. Trevejo-Nunez, E. Kincaid, T. Tamura, K. Takatsu, and J.D. Ernst. 2007. *Mycobacterium tuberculosis* infects dendritic cells with high frequency and impairs their function in vivo. *J. Immunol.* 179:2509–2519.

39. Egen, J.G., A.G. Rothfuchs, C.G. Feng, N. Winter, A. Sher, and R.N. Germain. 2008. Macrophage and T cell dynamics during the development and disintegration of mycobacterial granulomas. *Immunity.* 28:271–284.

40. Ramachandra, L., E. Noss, W.H. Boom, and C.V. Harding. 2001. Processing of *Mycobacterium tuberculosis* antigen 85B involves intraphagosomal formation of peptide–major histocompatibility complex II complexes and is inhibited by live bacilli that decrease phagosome maturation. *J. Exp. Med.* 194:1421–1432.

41. Ting, L.M., A.C. Kim, A. Cattamanchi, and J.D. Ernst. 1999. *Mycobacterium tuberculosis* inhibits IFN-gamma transcriptional responses without inhibiting activation of STAT1. *J. Immunol.* 163:3898–3906.

42. Bodnar, K.A., N.V. Serbina, and J.L. Flynn. 2001. Fate of *Mycobacterium tuberculosis* within murine dendritic cells. *Infect. Immun.* 69:800–809.

43. Noss, E.H., C.V. Harding, and W.H. Boom. 2000. *Mycobacterium tuberculosis* inhibits MHC class II antigen processing in murine bone marrow macrophages. *Cell. Immunol.* 201:63–74.

44. Pancholi, P., A. Mirza, N. Bhardwaj, and R.M. Steinman. 1993. Sequestration from immune CD4+ T cells of mycobacteria growing in human macrophages. *Science.* 260:984–986.

45. Hmama, Z., R. Gabathuler, W.A. Jefferies, G. de Jong, and N.E. Reiner. 1998. Attenuation of HLA-DR expression by mononuclear phagocytes infected with *Mycobacterium tuberculosis* is related to intracellular sequestration of immature class II heterodimers. *J. Immunol.* 161:4882–4893.